Steric and Allosteric Effects of Fatty Acids on the Binding of Warfarin to Human Serum Albumin Revealed by Molecular Dynamics and Free Energy Calculations

Shin-ichi Fujiwara* and Takashi Amisaki

Department of Biological Regulation, Faculty of Medicine, Tottori University; 86 Nishi-cho, Yonago 683–8503, Japan.
Received January 21, 2011; accepted April 5, 2011; published online April 6, 2011

Human serum albumin (HSA) binds with drugs and fatty acids (FAs). This study was initiated to elucidate the relationship between the warfarin binding affinity of HSA and the positions of bound FA molecules. Molecular dynamics simulations of 11 HSA-warfarin-myristate complexes were performed. HSA-warfarin binding free energy was then calculated for each of the complexes by the molecular mechanics-Poisson–Boltzmann surface area (MM-PBSA) method. The results indicated that the magnitude of the binding free energy was smaller in HSA-warfarin complexes that had 4 or more myristate molecules than in complexes with no myristate molecules. The unfavorable effect on the HSA-warfarin binding affinity was caused sterically by the binding of a myristate molecule to the FA binding site closest to the warfarin binding site. On the other hand, the magnitude of HSA-warfarin binding free energy was largest when 3 myristate molecules were bound to the high-affinity sites. The strongest HSA-warfarin binding was attributable to favorable entropic contribution related to larger atomic fluctuations of the amino acid residues at the warfarin binding site. In the binding of 2 myristate molecules to the sites with the highest and second-highest affinities, allosteric modulation that enhanced electrostatic interactions between warfarin and some of the amino acid residues around the warfarin binding site was observed. This study clarified the structural and energetic properties of steric/allosteric effects of FAs on the HSA-warfarin binding affinity and illustrated the approach to analyze protein–ligand interactions in situations such that multiple ligands bind to the other sites of the protein.

Key words human serum albumin; molecular dynamics simulation; binding free energy; multiple binding site; warfarin; fatty acid

Human serum albumin (HSA) is the most abundant protein in blood plasma. It serves as a transport protein for several endogenous compounds such as nonesterified fatty acids (FAs), and is also capable of binding many commonly used drugs. Drug binding to HSA can result in a prolonged *in vivo* half-life. Thus, the binding of drugs to HSA is one of the most important factors determining their pharmacokinetics.[1)]

HSA consists of 585 amino acids and has a molecular mass of 66500 Da. The structure of HSA consists of 3 homologous domains (domains I—III), each of which is divided into 2 subdomains, A and B, having 6 and 4 α-helices, respectively (Fig. 1).[2—4)] Multiple ligand-binding sites have been reported for these subdomains. Two primary drug-binding sites, I (the warfarin binding site, located in subdomain IIA) and II (the indole-benzodiazepine site, located in subdomain IIIA), have received particular attention because of their high drug-binding affinity.[5,6)] Seven FA binding sites have been also reported as common sites for medium- and long-chain FAs,[7)] as well as for monosaturated and polyunsaturated FAs.[8)] Detailed studies on these sites have been performed by using X-ray crystallography,[7—12)] site-directed mutagenesis,[13—15)] and ^{13}C-NMR spectroscopy.[16,17)]

Under normal physiological conditions, HSA binds with approximately 0.1—2 mol FA per mol protein.[18)] The FA/HSA molar ratio can increase up to six during fasting or maximum exercise,[19,20)] or in patients with diabetes.[21)] In the high-ratio state, FA may affect the interactions between HSA and drugs because some FA binding sites overlap with drug binding sites I and II.[12)] Numerous studies have shown that drug binding to HSA can be modulated competitively or even cooperatively, by simultaneous binding of FAs.[1,12,22—27)] In the case of HSA-warfarin binding, it was reported that the addition of 2—4 mol of long-chain FAs per mol of HSA markedly increased the binding affinity of warfarin to HSA, whereas further addition of FAs decreased the affinity.[24)]

The effects of FAs on HSA-drug binding have been analyzed from the standpoint of the molecular structure. The binding of FA molecules to HSA can cause a relative rearrangement at the I—II and II—III domain interfaces[9,28)] and conformational changes of the side chains of drug binding site I.[12)] However, these studies are based on the HSA structures with all FA-accommodating sites being occupied by FA molecules. To date, there are no published works concerning the individual effect of FA binding to each site on

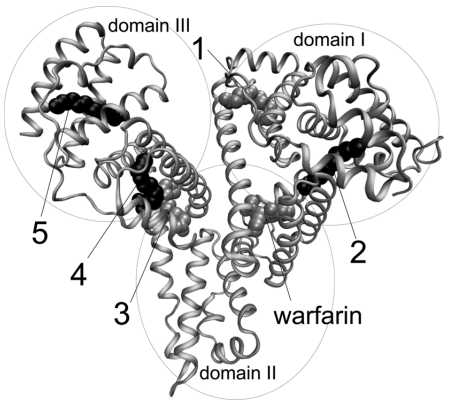

Fig. 1. Ribbon Model of the HSA-Wf-Myr Complex Derived from X-Ray Crystallography (PDB Entry 1H9Z)

HSA is composed of 3 homologous domains, I—III, each of which is divided into 2 subdomains, A and B. The 5 myristate molecules are shown in black (high-affinity FA binding sites) or gray (low-affinity FA binding sites) in a space-filling representation. Numbering of the FA binding sites was sourced from Bhattacharya *et al.*[7)]

* To whom correspondence should be addressed. e-mail: fujiwara@med.tottori-u.ac.jp

HSA-drug binding.

The present study was undertaken to elucidate the relationship between the HSA-drug binding affinity and the positions of bound FA molecules. In our previous study,[29] the binding free energy of a single palmitate or myristate molecule at each FA binding site was calculated using molecular dynamics (MD) simulations and the subsequent binding free energy calculations by the molecular mechanics Poisson–Boltzmann surface area (MM-PBSA)[30] method. The results of the calculations were consistent with the experimentally determined FA binding affinities.[29] Using a similar approach, we calculated the binding free energies of a drug (warfarin) to HSA with FA molecules bound to various positions on HSA. Unlike conventional MM-PBSA applications which analyze simple protein–ligand binding systems, this study deals with the systems such that multiple ligands bind to the other sites of the protein.

We present the results of the HSA-warfarin binding free energy calculations for a series of HSA-warfarin-myristate (HSA-Wf-Myr) complexes. Three effects of the bound FA molecules are reported. One is the effect due to a single FA molecule, which causes unfavorable steric interactions in HSA-warfarin binding. Next is the allosteric effect that causes an increase in atomic fluctuations at drug binding site I by the binding of FA molecules, which is related to the entropic contribution. The other is the allosteric effect that strengthens the favorable electrostatic contribution in HSA-warfarin binding, which is induced by simultaneous bindings of 2 FA molecules to the specific FA binding sites.

Experimental

Starting Structure of HSA-Wf-Myr Complex The initial coordinates of the HSA-Wf-Myr complex were obtained from the Protein Data Bank (PDB)[31] (PDB entry 1H9Z, structure resolution 2.5 Å). In the original structure, myristate molecules were bound to 6 of the 7 FA binding sites, and warfarin was bound to the other FA binding site, which is coincident with drug binding site I.[12] In this study, 1 myristate molecule that bound to subdomain IIB was removed because the binding of FAs to this site was much weaker than that to the other sites.[9,17,29] Therefore, 1 warfarin and 5 myristate molecules were included in the subsequent MD simulations (Fig. 1).

Preparation of Multiple HSA-Wf-Myr Complexes The 5 FA binding sites have different FA binding affinities, which can be ranked as follows: $5>4>2\gg1\approx3$, as reported previously.[17,29] FA binding sites 5, 4, and 2 are high-affinity sites, and 1 and 3 are low-affinity sites (Fig. 1). On this basis, FA-bound or unbound systems were prepared. For the states where 2 myristate molecules were bound to HSA, for example, 3 HSA-Wf-Myr complexes were prepared in which 2 myristate molecules were bound to FA binding sites 4 and 2 (2Myr42), 5 and 2 (2Myr52), or 5 and 4 (2Myr54). Similarly, for the states where 4 myristate molecules bind to HSA, 2 complexes were prepared in which 3 myristate molecules occupied all 3 high-affinity sites and 1 myristate molecule binds to FA binding sites 1 (4Myr1) or 3 (4Myr3). Consequently, 11 complexes were prepared (Table 1).

Molecular Dynamics Simulations of a Series of HSA-Wf-Myr Complexes A series of MD calculations were performed using the AMBER9 package (University of California, San Francisco, U.S.A.). The LEaP module was used to construct a model of the 5Myr complex. The sander and particle-mesh Ewald molecular dynamics (pmemd) modules were used for energy minimization and MD calculations, respectively. The parm94 force field[32] was used for modeling the HSA system. The force fields of myristate and warfarin were generated by the antechamber module, based on the general AMBER force field (GAFF).[33] Following *ab initio* optimization of the myristate or warfarin molecule at the HF/6-31G* level by Gaussian 03 Revision A.1 (Gaussian Inc., Pittsburgh, U.S.A.), a restrained electrostatic potential fit procedure[34] was used as the charge method in GAFF. Missing residues in the starting structure of HSA (residues 1, 2, 585) were added by the Build and Edit Protein tool in Discovery Studio version 1.5 (Accelrys Inc., San Diego, U.S.A.). After the addition of missing residues, missing atoms were added by the LEaP module. Energy minimization with constraints on the positions of non-hydrogen atoms was conducted for 500 steps. Na^+ counterions were placed by LEaP to neutralize the negative charges of the 5Myr complex system at neutral pH. A rectangular box of water was constructed using the TIP3P water model[35] with 15-Å buffering distance. The resulting systems contained 114673 atoms. The subsequent energy minimization and MD simulations were performed under periodic boundary conditions. For the system, 500 steps of energy minimization constraining the HSA, myristate, warfarin, and counterions were performed, followed by 500 steps of energy minimization with no constraints. After energy minimization, constant-volume MD calculations were performed for 200 ps, during which the temperature was increased from 0 to 310 K, followed by a total of 6-ns constant-pressure MD calculations. The nonbonded list was generated using an atom-based cutoff of 9 Å. The long-range electrostatic interactions were handled by the particle-mesh Ewald algorithm.[36] The time step of the MD simulations was set to 2.0 fs, and the SHAKE algorithm[37] was used to constrain bond lengths at their equilibrium values. Temperature and pressure were maintained using the weak-coupling algorithm[38] with coupling constants (τ_T and τ_P) of 1.0 ps (310 K, 1 atm). Coordinates were saved for analyses every 1 ps.

Table 1. HSA-Warfarin-Myristate Complexes Prepared in This Study

Number of myristate molecules	Position of myristate molecules[a]
0 (0Myr)	no
1 (1Myr)	5 (1Myr5)
	4 (1Myr4)
	2 (1Myr2)
2 (2Myr)	5, 4 (2Myr54)
	5, 2 (2Myr52)
	4, 2 (2Myr42)
3 (3Myr)	5, 4, 2
4 (4Myr)	5, 4, 2, 1 (4Myr1)
	5, 4, 2, 3 (4Myr3)
5 (5Myr)	5, 4, 2, 1, 3

a) Position number is according to Fig. 1. The abbreviation of each complex is shown in parentheses.

Multiple HSA-Wf-Myr complexes (Table 1) were obtained by removing the myristate molecules from a snapshot of the 5Myr complex at 6 ns. Starting with each HSA-Wf-Myr complex structure, additional 6-ns MD simulations were performed under the same conditions described above.

The MD simulations and the subsequent MM-PBSA calculations were run on an in-house PC cluster composed of 16 nodes (AMD Opteron 2.4 GHz dual core, 4 GB DDR memory) with a gigabit Ethernet interconnection. Trajectory analyses were performed using the ptraj module. Structural diagrams were prepared by Visual Molecular Dynamics (VMD; version 1.8.6).[39]

Binding Free Energy Calculations by MM-PBSA The binding free energy (ΔG_{bind}) of warfarin to HSA in each HSA-Wf-Myr system was calculated as follows:

$$\Delta G_{bind} = G^{HSA\text{-}Wf\text{-}Myr} - G^{HSA\text{-}Myr} - G^{Wf} \quad (1)$$

where $G^{HSA\text{-}Wf\text{-}Myr}$, $G^{HSA\text{-}Myr}$, and G^{Wf} are the free energies of the HSA-Wf-Myr complex, HSA-myristate complex, and warfarin, respectively. The free energy (G) of each state can be calculated as follows:

$$G = E_{MM} + G_{PB} + G_{SA} - TS \quad (2)$$

$$E_{MM} = E_{vdw} + E_{ele} + E_{int} \quad (3)$$

where E_{MM} is the molecular mechanical energy, G_{PB} is the polar contribution to the solvation free energy, G_{SA} is the nonpolar contribution to the solvation free energy, and TS is the entropic contribution of the solute (T: absolute temperature, S: entropy). E_{MM} was obtained by summing the contributions of internal energies including bond, angle, and torsional angle energies (E_{int}), Coulomb energy (E_{ele}), and van der Waals energy (E_{vdw}), using the same force field as that of the MD simulations with no cutoff. G_{PB} was calculated using the DelPhi program[40] with PARSE[41] atom radii and standard AMBER94 charges[32] for amino acids. A grid size of 0.5 Å was used to solve the Poisson–Boltzmann equation, and the dielectric constants inside and outside the molecule were 1.0 and 80.0, respectively. To obtain the residue-based decomposition of the G_{PB} term, G_{PB} was also calculated using the PBSA module in AMBER10 (University of California, San Francisco, U.S.A.) under the same conditions used for DelPhi. G_{SA} was calculated

using a solvent accessible surface area (*SASA*) as follows:

$$G_{SA}=\gamma\times SASA+b \quad (4)$$

SASA was computed with the molsurf module in AMBER9 by using a probe radius of 1.4 Å. The surface tension proportionality constant (γ) and the free energy of nonpolar solvation for a point solute (b) were set to 0.00542 kcal/mol/Å^2 and 0.92 kcal/mol, respectively.[41] The entropy contribution from vibrational motion was obtained by normal mode analysis.[42] Because normal mode analysis is computationally expensive, only drug binding site I (residues 197—297) and warfarin were retrieved from an MD snapshot for each HSA-Wf-Myr complex and were used for the calculation. The snapshots were energy-minimized with a distance-dependent dielectric function ($\varepsilon=4R_{ij}$) until the root mean-square of the elements of the gradient vector was $<10^{-4}$ kcal/mol/Å. Then, the frequencies of the vibrational modes were computed at 300 K for the minimized structures using a harmonic approximation of the energies.

For the MM-PBSA calculations of the energy and the entropic components, 500 snapshots extracted from a single trajectory of the HSA-Wf-Myr complex were taken at time intervals of 8 ps from the 4-ns production runs (8—12 ns). The binding free energy was calculated as follows:

$$\Delta G_{bind}=\langle G^{HSA\text{-}Wf\text{-}Myr}-G^{HSA\text{-}Myr}-G^{Wf}\rangle \quad (5)$$

The change in internal energies (ΔE_{int}) equals zero in the binding free energy calculation by Eq. 5, as the internal energies of the complex and the separated parts are calculated from the same trajectory.

Results and Discussion

Warfarin as the Target Drug in This Study Warfarin is the most widely used oral anticoagulant drug for patients with venous thrombosis or pulmonary embolism, and it binds to HSA at a high proportion.[43] Compared with other drugs, there is a plethora of experimental data regarding HSA-warfarin binding constants under various FA/HSA molar ratios,[23,24] as well as X-ray structures of HSA-warfarin complexes.[11,15] As discussed below, the experimental data were compared with the calculated HSA-warfarin binding free energies of the 11 HSA-Wf-Myr complexes for validation, followed by detailed structural comparisons among the complexes. Through the HSA-Wf-Myr binding system, this study illustrates the approach to analyze protein–ligand binding systems such that multiple ligands bind to the other sites of the protein. This approach may be applicable to the binding of multiple ligands to other proteins with multiple binding sites, as well as to the binding of other drugs to HSA.

Both warfarin and FA can bind to drug binding site I on HSA.[12] However, warfarin was observed to displace an FA molecule in the X-ray structure (Fig. 1),[8] indicating that the binding affinity of warfarin at drug binding site I is higher than that of FA. It has been also reported that the binding affinity of an FA molecule at the site is much lower than that at the other FA binding sites.[9,17,29] Competitive binding of warfarin and myristate at drug binding site I was therefore not considered in this study.

Root Mean Square Deviation of HSA-Warfarin-Myristate Complex Figure 2 shows the root mean square deviations (RMSDs) of C_α atoms from the X-ray structure in HSA-Wf-Myr complex systems. In the 5Myr system, RMSD values of all C_α atoms reached a plateau at about 2 ns. The RMSD values of C_α atoms belonging to drug binding site I were $\leq$2.0 Å, indicating that no significant structural drift from the X-ray structure occurred at the site during the MD simulations. Additional 6-ns MD simulations of the other complex systems also showed that no significant structural drift occurred at drug binding site I and that RMSD values reached a plateau at about 8 ns. We used 8- to 12-ns trajectories in the following binding free energy calculations.

HSA-Warfarin Binding Free Energies of HSA-Wf-Myr Complexes Table 2 summarizes the calculated HSA-warfarin binding free energy components of 11 HSA-Wf-Myr complexes. The binding free energies of warfarin to HSA with 0 (0Myr), 1 (1Myr5; 1 myristate molecule is bound to the highest FA binding site 5), 3 (3Myr; 3 myristate molecules are bound to HSA), and 5 (5Myr) myristate molecules were compared to analyze the effect of the number of bound FA molecules. The magnitude of the binding free energy was similar in the complexes with 0 or 1 myristate molecule, while it was larger (*i.e.*, the HSA-warfarin binding affinity was stronger) in that with 3 molecules, and smaller (*i.e.*, the HSA-warfarin binding affinity was weaker) in that with 5 molecules. This result coincides with the previous *in vitro* observations that the affinity constant of warfarin decreases under a high concentration of FAs (FA/HSA molar ratio

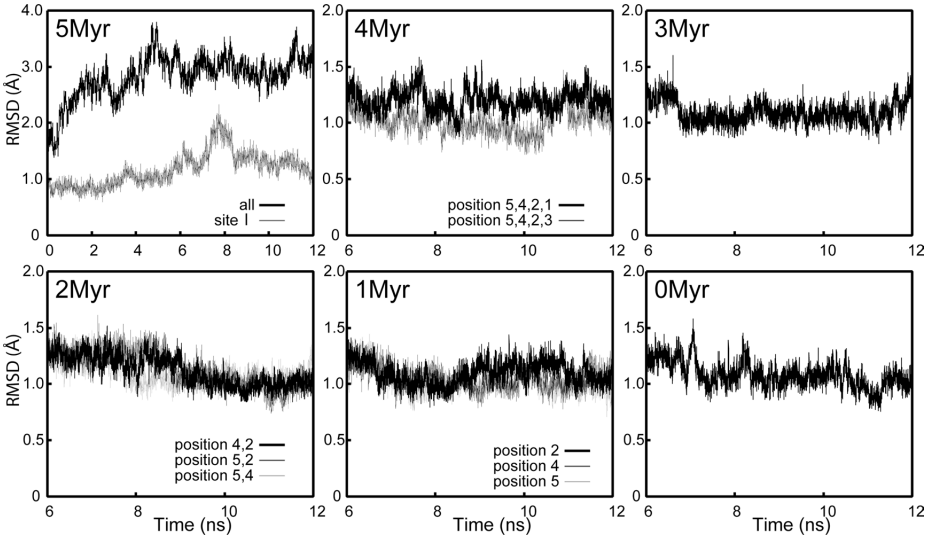

Fig. 2. Time Evolution of the RMSD of C_α Atoms from the X-Ray Structure

In the 5Myr complex (left upper), RMSDs of all C_α atoms (black line) and those belonging to drug-binding site I (gray line) are presented. In the other complex systems, RMSDs of C_α atoms belonging to drug-binding site I are presented.

Table 2. Calculated HSA-Warfarin Binding Free Energy Components for the 11 HSA-Wf-Myr Complexes by MM-PBSA (in Units of kcal/mol)[a)]

Complex	ΔE_{vdw}	ΔE_{ele}	ΔG_{SA}	ΔG_{PB}	ΔG_{PBele}[b)]	ΔG_{mmpbsa}[c)]	$T\Delta S$	ΔG_{bind}[d)]
0Myr	−39.0 (0.1)	−35.0 (0.3)	−5.1 (0.01)	59.3 (0.3)	24.4 (0.2)	−19.7 (0.2)	−13.5 (0.2)	−6.2 (0.3)
1Myr5	−39.3 (0.1)	−27.3 (0.2)	−5.1 (0.01)	51.9 (0.2)	24.6 (0.2)	−19.7 (0.2)	−14.0 (0.2)	−5.8 (0.3)
1Myr4	−38.7 (0.1)	−28.6 (0.2)	−5.1 (0.01)	53.7 (0.2)	25.1 (0.2)	−18.7 (0.2)	−15.2 (0.2)	−3.5 (0.3)
1Myr2	−34.1 (0.1)	−32.2 (0.4)	−5.0 (0.01)	56.8 (0.5)	24.6 (0.2)	−14.5 (0.2)	−12.7 (0.3)	−1.7 (0.3)
2Myr54	−38.1 (0.1)	−28.9 (0.2)	−5.1 (0.01)	50.9 (0.2)	22.0 (0.2)	−21.3 (0.2)	−15.0 (0.2)	−6.2 (0.3)
2Myr52	−35.8 (0.1)	−30.0 (0.2)	−5.1 (0.01)	52.9 (0.2)	22.9 (0.2)	−18.0 (0.2)	−11.0 (0.3)	−6.9 (0.3)
2Myr42	−36.8 (0.1)	−28.6 (0.2)	−5.0 (0.01)	51.4 (0.3)	22.7 (0.2)	−19.1 (0.2)	−14.4 (0.2)	−5.0 (0.3)
3Myr	−34.8 (0.1)	−32.4 (0.3)	−5.1 (0.01)	53.8 (0.3)	21.4 (0.2)	−18.3 (0.2)	−9.5 (0.3)	−8.8 (0.3)
4Myr1	−35.0 (0.1)	−32.5 (0.4)	−5.1 (0.01)	53.7 (0.4)	21.2 (0.2)	−18.9 (0.2)	−13.6 (0.3)	−5.3 (0.3)
4Myr3	−34.9 (0.1)	−26.2 (0.3)	−4.8 (0.01)	46.6 (0.3)	20.4 (0.2)	−19.3 (0.2)	−16.6 (0.2)	−2.7 (0.3)
5Myr	−38.4 (0.1)	−28.2 (0.3)	−5.1 (0.01)	53.2 (0.2)	25.0 (0.2)	−18.5 (0.2)	−13.6 (0.2)	−5.0 (0.3)

a) Number in parentheses is the standard error of the mean. *b*) $\Delta G_{PBele}=\Delta E_{ele}+\Delta G_{PB}$. This is the electrostatic component of the binding free energy. *c*) $\Delta G_{mmpbsa}=\Delta E_{ele}+\Delta E_{vdw}+\Delta G_{SA}+\Delta G_{PB}$. This is the enthalpic component of the binding free energy. *d*) $\Delta G_{bind}=\Delta G_{mmpbsa}-T\Delta S$. This was calculated according to Eq. 5.

of ≥5).[24)] The magnitude in the 5Myr complex was 1.2 kcal/mol lower than that of the 0Myr complex. The value of 1.2 kcal/mol corresponds to 7.5-fold of the affinity constant.

Next, to analyze which of the high-affinity sites influence HSA-warfarin binding, the binding free energies of the 3 1Myr complexes were compared (Table 2). Compared with the 1Myr5 complex, the magnitude of the binding free energy was smaller in the complex in which a myristate molecule was bound to FA binding site 4 (1Myr4) or 2 (1Myr2). In particular, a 4.1-kcal/mol difference in HSA-warfarin binding free energy was observed between the 1Myr2 and 1Myr5 complexes, indicating that the binding of a myristate molecule at FA binding site 2 influences HSA-warfarin binding unfavorably. Interestingly, the unfavorable effect was alleviated when another myristate molecule was bound to FA binding site 4 (2Myr42) or 5 (2Myr52) of the 1Myr2 complex (Table 2). Compared with the 0Myr complex, the magnitude of the binding free energy was equal in 2Myr54 complex (−6.2 kcal/mol), or larger in the 2Myr52 complex (−6.9 kcal/mol).

The other HSA-Wf-Myr complexes in which more than 3 myristate molecules are bound to HSA were also compared (Table 2). The magnitude of the binding free energy was larger in the 3Myr complex than in the 4Myr and 5Myr complexes. In comparison with the 4Myr complexes, the magnitude was larger when a myristate molecule was bound to FA binding site 1 rather than to site 3. FA binding sites 1 and 2 belong to domain I, while sites 3, 4, and 5 belong to domain III (Fig. 1). Thus, the resulting data suggested that the magnitude of the HSA-warfarin binding free energy tends to be larger when FA molecules are bound to domain I and III equivalently.

The proportion of each HSA-Wf-Myr complex (Table 1) under various FA/HSA molar ratios can be estimated from the FA binding affinity to each FA binding site, assuming that an FA molecule binds to each FA binding site independently. The FA binding affinity can be ranked as $5>4>2\gg1\approx3$.[17,29)] Accordingly, the proportion of HSA-Wf-Myr complexes in which FA binding site 5 is occupied by a myristate molecule will be very large, while the proportion of the 1Myr2 complex (most unfavorable HSA-warfarin binding) will be small. In fact, it was reported that HSA-warfarin binding affinity was not decreased significantly between an FA/HSA molar ratio of 0 and 1.[23,24)] On the other hand, Vorum and Honoré reported that HSA-warfarin binding affinity was increased at an FA/HSA molar ratio of 2—4.[24)] Within this range, the proportion of the 2Myr54, 2Myr52, and 3Myr complexes will be large because FA binding sites 5, 4, and 2 are high-affinity sites.[17,29)] As discussed above, the HSA-warfarin binding affinity was stronger in the 2Myr52 and 3Myr complexes than that in the 0Myr complex (Table 2). This implied that the increase in the HSA-warfarin binding affinity reported previously might have relevance to the proportion of these complexes.

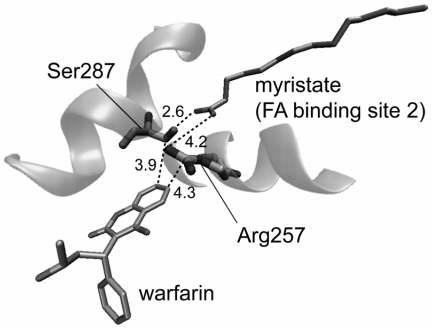

Fig. 3. Positions of Warfarin, Myristate Bound to FA Binding Site 2, Arg257, and Ser287 in the X-Ray Structure of the HSA-Wf-Myr Complex (PDB Entry 1H9Z)

The shortest distances between the non-hydrogen atoms of warfarin/myristate and these residues are presented (in units of Å).

Structural and Energetic Bases of the Binding of a Myristate Molecule to FA Binding Site 2 on HSA-Warfarin Binding As discussed above, the binding of warfarin to HSA was highly influenced by the binding of a myristate molecule to FA binding site 2 (Table 2). Among the 5 FA binding sites, site 2 is closest to drug binding site I (Fig. 1). Figure 3 depicts the positions of warfarin and myristate bound to FA binding site 2 in the original X-ray structure of the HSA-Wf-Myr complex (PDB entry 1H9Z).[11)] Warfarin made direct contacts with the side chains of Arg257 and Ser287, which in turn were in direct contact with a myristate molecule at FA binding site 2 (Fig. 3). The shortest distances between the non-hydrogen atoms of warfarin/myristate and these residues were ≤4.3 Å. Taking the hydrogen atoms into account, steric interactions between warfarin and the side chains, following the binding of a myristate molecule at FA binding site 2, were expected. Actually, in almost all HSA-Wf-Myr complexes with a myristate molecule bound to FA

binding site 2, the van der Waals energy contribution, ΔE_{vdw}, was larger (*i.e.*, the contribution was unfavorable) than that of the complexes without a myristate molecule at the site (Table 2). On the other hand, electrostatic component of the binding free energy, ΔG_{PBele} (=*i.e.*, $\Delta E_{ele}+\Delta G_{PB}$) did not differ significantly whether or not a myristate molecule binds to FA binding site 2. This indicated that in HSA-warfarin binding, the binding of a myristate molecule to the site was unfavorable in terms of the van der Waals energy contribution.

Relationship between HSA-Warfarin Binding Free Energy and Atomic Fluctuations at Drug Binding Site I Influence of the binding of myristate molecules on HSA-warfarin binding free energy was further analyzed on the point of local protein mobility. Figure 4 shows the comparison of the time-averaged root-mean-square fluctuation (RMSF) for each residue at drug binding site I along the sequence derived from the 8- to 12-ns MD simulations. We focused on the region of amino acid residues 190—260, because some of the amino acid residues (Lys195, Lys199, Phe211, Trp214, Arg218, Arg222, His242, and Arg257) in this region have been reported to alter the binding affinity of site I drugs.[13,14] In comparison with the 0Myr complex, the RMSF values were higher at almost all residues in the 1Myr2 complex. This uniform upward shift was observed only in the complex, indicating that drug binding site I of the 1Myr2 complex fluctuates more than those of the other complexes. Although the fluctuations in the 1Myr2 complexes caused relatively favorable entropic contribution ($T\Delta S$), they also caused more unfavorable enthalpic contribution, ΔG_{mmpbsa} (=*i.e.*, $\Delta E_{vdw}+\Delta G_{PBele}$). When another myristate molecule was bound to FA binding site 4 or 5 in addition to site 2, the RMSF values were smaller than those of the 1Myr2 complex. Correspondingly, the magnitude of the enthalpic contribution in HSA-warfarin binding free energy of the 2Myr42 or 2Myr52 complex was larger (*i.e.*, the HSA-warfarin binding affinity was stronger) than that of the 1Myr2 complex (Table 2). In HSA-Wf-Myr complexes where the magnitude of the enthalpic contribution was smaller (≥1.0 kcal/mol) than that in the 0Myr complex, the RMSF values of residues 210—230 and/or residues 230—260 tended to be larger than those in the 0Myr complex (residues 210—230: 1Myr2, 2Myr52, and 3Myr complexes; residues 230—260: 1Myr2, 1Myr4, 4Myr1, 3Myr, and 5Myr complexes). This suggested that the unfavorable enthalpic contribution in the HSA-warfarin binding affinity is in part due to the greater fluctuations observed in the HSA-Wf-Myr complexes, especially when one of the myristate molecules bound to FA binding site 2. On the other hand, the 2Myr52 and 3Myr complexes indicated strong HSA-warfarin affinity due to favorable entropic contribution (Table 2). In these complexes, the patterns of the RMSF values at residues 200—280 were similar (Fig. 4), suggesting that these residues were relevant to HSA-warfarin binding in terms of entropic contribution.

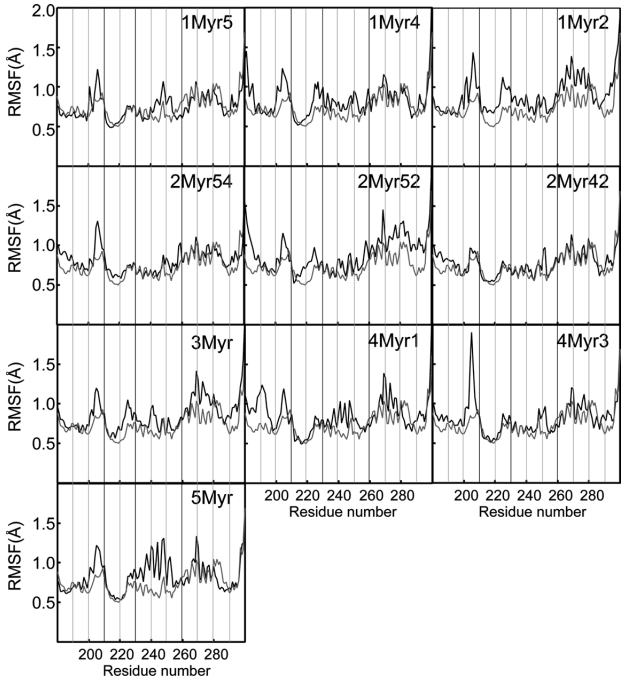

Fig. 4. Comparison of the RMSF of C_α Atoms Along the Sequence Derived from the 8- to 12-ns MD Simulations in the 0Myr Complex (Gray Line) and the Other HSA-Wf-Myr Complexes (Black Line)

Comparison of Two Methods for Calculating Electrostatic Component of the Binding Free Energy Electrostatic component of the binding free energy (ΔG_{PBele}) was decomposed by residue, as described below. The PBSA module in AMBER10 was used for this purpose, because no other program based on the DelPhi program was available for residue-based decomposition of the G_{PB} term. Compared with the calculated HSA-warfarin binding free energies of the 0Myr complex including the entropic term, the values were −6.2 and −15.4 kcal/mol for DelPhi and PBSA, respectively. Judging from the experimental HSA-warfarin binding free energy of approximately −7.6 to −6.6 kcal/mol, calculated from the affinity constants,[23,44,45] the G_{PB} term calculated by DelPhi was more accurate than that determined by PBSA in this study. However, the ΔG_{PBele} values computed for the 11 complexes by PBSA were well correlated with those calculated by DelPhi (Fig. 5). Thus, the ΔG_{PBele} values decomposed by residue using PBSA were comparable between each HSA-Wf-Myr complex with respect to rank order.

Structural and Energetic Bases of the Binding of 2 Myristate Molecules to FA Binding Sites 5 and 4 on HSA-Warfarin Binding The 2Myr54 complex had the highest

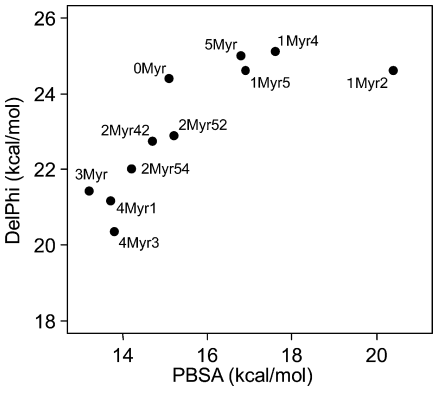

Fig. 5. Comparison of ΔG_{PBele} Values in the 11 HSA-Wf-Myr Complexes Computed by the PBSA Module with Those Computed by the DelPhi Program

Pearson and Kendall correlation coefficients between them were 0.800 and 0.734, respectively (n=11).

Table 3. Residue-Based Decomposition of HSA-Warfarin Binding Free Energy for the Electrostatic Component, $\Delta G_{\mathrm{PBele}}$ (in Units of kcal/mol)[a,b]

Residue	0Myr	1Myr			2Myr			3Myr	4Myr		5Myr
		2	4	5	42	52	54		1	3	
Glu153	0.11	1.46	0.51	0.31	0.12	0.23	0.32(9)	0.08	0.23	0.26(7)	0.13
Lys195	−0.21	−0.09	−0.35	−0.06	−0.11	−0.01	−0.06(8)	−0.04	−0.12	−0.09(6)	−0.15
Gln196	−0.03	0.01	−0.01	−0.04	−0.02	−0.01	−0.01(8)	−0.02	−0.07	−0.02(5)	−0.05
Lys199	2.48	2.21	2.88	3.20	2.40	2.33	2.32(5)	2.22	2.18	1.21(1)	2.52
Phe211	0.91	0.24	0.64	0.68	1.06	0.72	0.84(8)	0.73	0.86	0.58(2)	0.83
Trp214	0.51	0.07	0.40	0.60	0.48	0.53	0.53(9)	0.45	0.40	0.17(2)	0.34
Arg218	1.02	0.34	0.92	1.38	1.26	1.36	1.25(7)	1.43	1.02	0.69(2)	1.11
Arg222	0.27	0.75	0.15	1.06	0.26	1.30	0.01(1)	0.59	0.05	0.11(3)	1.10
Asp237	−0.16	0.06	−0.13	−0.39	0.02	−0.04	−0.18(3)	0.02	0.13	−0.22(2)	−0.10
Leu238	0.22	0.07	0.33	0.17	0.20	0.24	0.23(8)	0.22	0.18	0.19(4)	0.31
His242	1.47	0.73	1.45	1.15	0.64	0.34	0.13(1)	0.19	0.24	1.55(11)	1.52
Arg257	1.50	3.24	2.41	1.84	1.72	1.37	2.03(8)	1.49	1.10	2.42(10)	1.72
Ser287	−0.39	0.43	−0.50	−0.39	−0.33	−0.26	−0.54(1)	−0.23	−0.24	−0.45(3)	−0.42
Ile290	1.42	0.91	1.42	1.16	1.20	1.10	1.34(7)	1.08	1.16	1.42(9)	1.39
Ala291	1.29	1.12	1.42	1.26	1.28	1.26	1.31(7)	1.31	1.37	1.49(11)	1.27
Glu292	1.87	1.29	1.55	1.62	0.95	1.30	1.40(8)	0.93	1.05	0.99(3)	1.11
Asp451	0.52	0.06	0.28	0.07	0.14	0.13	0.12(4)	0.04	0.17	0.37(9)	0.47
Sum[c]	4.96	7.82	6.22	6.54	5.33	5.95	4.94	5.38	4.52	4.54	6.04

a) Gln196 and the residues with absolute values of more than 0.3 kcal/mol among one of the complexes are shown. *b*) The numbers in parentheses in the 2Myr54 and 4Myr3 complexes represent the rank of the favorable electrostatic contribution for each residue. *c*) Decomposed electrostatic components of Gln196, Lys199, Arg222, Arg237, Arg257, Ser287, and Ala291 were summed for each complex.

Table 4. Atomic Distances between Residues Relevant to Electrostatic Contribution of HSA-Warfarin Binding for the Averaged Complexes (in Units of Å)

Atom pair	0Myr	1Myr			2Myr			3Myr	4Myr		5Myr
		5	4	2	54	52	42		1	3	
Gln196@C_δ-Lys199@N_ζ	7.1	5.9	7.2	7.7	7.9	6.7	7.4	6.9	6.7	6.5	6.6
Gln196@C_δ-Arg257@C_ζ	9.0	7.9	9.1	7.7	12.2	10.3	9.7	10.5	9.7	12.6	9.2
Lys199@N_ζ-Arg257@C_ζ	8.2	8.9	9.2	9.4	7.8	8.2	9.0	8.0	9.2	7.4	8.0
Arg257@N-Arg237@O	7.5	6.9	7.9	7.3	7.3	7.9	7.7	7.9	7.6	7.4	7.9
Arg257@C_ζ-Ser287@C_α	5.5	5.5	5.5	9.8	5.5	5.4	5.5	5.7	5.4	5.5	5.6
Arg257@C_ζ-Ala291@C_α	5.6	5.4	5.5	9.5	5.8	5.6	5.6	5.6	5.7	5.9	5.7
Arg222@C_ζ-Ala291@O	3.4	3.2	3.6	5.3	3.4	3.2	3.3	3.3	3.3	3.6	3.5

enthalpic contribution ($\Delta G_{\mathrm{mmpbsa}} = -21.3$ kcal/mol) in HSA-warfarin binding among the 11 complexes. In the complex, the electrostatic component of the binding free energy ($\Delta G_{\mathrm{PBele}}$) was smaller (*i.e.*, the contribution was more favorable) than those of the other 2Myr complexes (Table 2). The same was applied for the 4Myr3 complex, implying that there are common characteristics of these complexes with respect to favorable electrostatic contributions. The interactions between warfarin and amino acid residues were therefore analyzed. Table 3 shows residue-based decomposition of the HSA-warfarin binding free energy for electrostatic contribution. The rank of the contribution in the 2Myr54 and 4Myr3 complexes is depicted in this table, because differences between the complexes indicating the favorable electrostatic contribution and the other complexes are important. In both 2Myr54 and 4Myr3 complexes, Lys199, Arg222, Asp237, and Ser287 made favorable electrostatic contributions, whereas Arg257 and Ala291 contributed unfavorably. Of these residues, Lys199, Arg222, Asp237, and Arg257 have been reported to alter the binding affinity of site I drugs.[13,14]

The structure of each HSA-Wf-Myr complex was also compared with the others. The time-averaged structure was obtained from the 8- to 12-ns trajectory data of each complex. All averaged structures were fitted on the position of C_α atoms at subdomain IIA, and the RMSF of non-hydrogen atoms among the structures was calculated for each residue. Residues having RMSF values of more than 1.0 Å were Gln196, Arg197, Gln204, Arg209, Lys240, Val241, Leu250, and Leu251. Among the residues, direction of the side chain of Gln196 was quite different between the 2Myr54/4Myr3 complex and the others (Fig. 6). However, the electrostatic contribution of Gln196 on HSA-warfarin binding was less

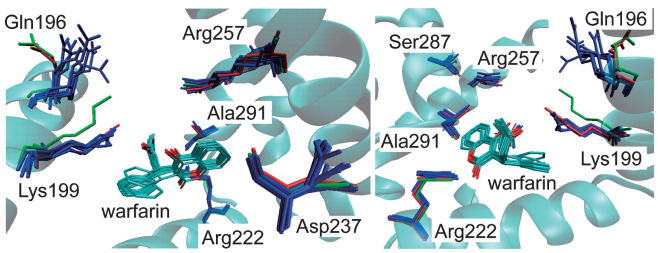

Fig. 6. Comparison of Average Structures among the 11 HSA-Wf-Myr Complexes

Gln196, Lys199, Arg222, Arg237, Arg257, Ser287, and Ala291 of 2Myr54, 4Myr3, and the other complexes are shown in red, green, and blue, respectively. Oxygen atoms of warfarin are shown in red. For clarity, the hydrogen atoms and the other residues are not displayed.

than 0.1 kcal/mol in all complexes (Table 3), suggesting that the residue indirectly affects the favorable electrostatic contribution of HSA-warfarin binding. Figure 6 shows superimposed structures of the 11 HSA-Wf-Myr complexes. Although Gln196, Lys199, and Arg257 were located close to each other in all of the complexes, their relative positions in the 2Myr54 complex were slightly different from the other complexes. Table 4 shows atomic distances between residues relevant to the electrostatic contribution of HSA-warfarin binding. The distance between Gln196 and Lys199/Arg257 was longer, and consequently, the distance between Lys199 and Arg257 was shorter in the 2Myr54 complex. On the other hand, the relative positions of the other residues, Arg222, Arg237, Ser287, and Ala291, were not different among the complexes (Table 4). When the electrostatic component of the binding free energy decomposed by residues was summed for these residues, it was small (*i.e.*, the contribution was favorable) in the 2Myr54 complex (Table 3). In summary, it was suggested that the binding of 2 myristates to FA binding sites 5 and 4 could change the interaction between Lys199 and Arg257 by changing the direction of the side chain of Gln196, resulting in more favorable electrostatic contribution of HSA-warfarin binding.

Conclusion

The present study revealed the steric and allosteric effects of FA molecules on the HSA-warfarin binding by using the MD simulations and the subsequent free energy calculations. The unfavorable HSA-warfarin binding was attributable to the steric effect by the binding of a myristate molecule to FA binding site 2. It was indicated by the unfavorable contribution of van der Waals energy to the binding free energy. The unfavorable HSA-warfarin binding was also attributable to the increase in the atomic fluctuations of the amino acid residues belonging to drug binding site I. On the other hand, when 3 FA molecules were bound to high-affinity FA binding sites, 5, 4, and 2, the HSA-warfarin binding affinity was highest among the 11 HSA-Wf-Myr complexes. The favorable HSA-warfarin binding was attributable to favorable entropic contribution related to larger atomic fluctuations at the warfarin binding site. When 2 FA molecules were bound to the highest and second-highest-affinity FA binding sites, 5 and 4, the enthalpic contribution of HSA-warfarin binding affinity was highest among the 11 HSA-Wf-Myr complexes. The favorable enthalpic contribution was attributable to the allosteric effect, which was indicated by the difference in the direction of the side chain of Gln196, accompanied by the binding of FA molecules to the sites.

The effect of change in the free drug concentration caused by changes in the HSA-drug binding affinity is generally considered to be of little clinical importance.[46] From the standpoint of the molecular level, however, it is also reasonable to expect that the changes in HSA-drug binding affinity by the binding of FAs observed in this study may influence, to a varying degree, the pharmacokinetics of drugs. Nonetheless, further investigation will be necessary to link the change in HSA-drug binding occurring at the molecular level with the macroscopic phenomenon. On this point, this work illustrated the approach to analyze protein-ligand binding systems such that multiple ligands bind to the other sites of the protein. This approach may be applicable to the binding of multiple ligands to other proteins with multiple binding sites, as well as to the binding of other drugs to HSA.

Acknowledgement This study was supported in part by Grants-in-Aid for Scientific Research from the Ministry of Education, Culture, Sports, Science and Technology of Japan.

References

1) Kragh-Hansen U., Chuang V. T. G., Otagiri M., *Biol. Pharm. Bull.*, **25**, 695—704 (2002).
2) He X. M., Carter D. C., *Nature* (London), **358**, 209—215 (1992).
3) Dockal M., Carter D. C., Rüker F., *J. Biol. Chem.*, **274**, 29303—29310 (1999).
4) Sugio S., Kashima A., Mochizuki S., Noda M., Kobayashi K., *Protein Eng.*, **12**, 439—446 (1999).
5) Sudlow G., Birkett D. J., Wade D. N., *Mol. Pharmacol.*, **11**, 824—832 (1975).
6) Sjöholm I., Ekman B., Kober A., Ljungstedt-Påhlman I., Seiving B., Sjödin T., *Mol. Pharmacol.*, **16**, 767—777 (1979).
7) Bhattacharya A. A., Grüne T., Curry S., *J. Mol. Biol.*, **303**, 721—732 (2000).
8) Petitpas I., Grüne T., Bhattacharya A. A., Curry S., *J. Mol. Biol.*, **314**, 955—960 (2001).
9) Curry S., Mandelkow H., Brick P., Franks N., *Nat. Struct. Biol.*, **5**, 827—835 (1998).
10) Curry S., Brick P., Franks N. P., *Biochim. Biophys. Acta*, **1441**, 131—140 (1999).
11) Petitpas I., Bhattacharya A. A., Twine S., East M., Curry S., *J. Biol. Chem.*, **276**, 22804—22809 (2001).
12) Ghuman J., Zunszain P. A., Petitpas I., Bhattacharya A. A., Otagiri M., Curry S., *J. Mol. Biol.*, **353**, 38—52 (2005).
13) Petersen C. E., Ha C. E., Curry S., Bhagavan N. V., *Proteins*, **47**, 116—125 (2002).
14) Watanabe H., Kragh-Hansen U., Tanase S., Nakajou K., Mitarai M., Iwao Y., Maruyama T., Otagiri M., *Biochem. J.*, **357**, 269—274 (2001).
15) Kragh-Hansen U., Watanabe H., Nakajou K., Iwao Y., Otagiri M., *J. Mol. Biol.*, **363**, 702—712 (2006).
16) Simard J. R., Zunszain P. A., Ha C. E., Yang J. S., Bhagavan N. V., Petitpas I., Curry S., Hamilton J. A., *Proc. Natl. Acad. Sci. U.S.A.*, **102**, 17958—17963 (2005).
17) Simard J. R., Zunszain P. A., Hamilton J. A., Curry S., *J. Mol. Biol.*, **361**, 336—351 (2006).
18) Fredrickson D. S., Gordon R. S. Jr., *J. Clin. Invest.*, **37**, 1504—1515 (1958).
19) Brodersen R., Andersen S., Vorum H., Nielsen S. U., Pedersen A. O., *Eur. J. Biochem.*, **189**, 343—349 (1990).
20) Bahr R., Høstmark A. T., Newsholme E. A., Grønnerød O., Sejersted O. M., *Acta Physiol. Scand.*, **143**, 105—115 (1991).
21) Paolisso G., Tataranni P. A., Foley J. E., Bogardus C., Howard B. V., Ravussin E., *Diabetologia*, **38**, 1213—1217 (1995).
22) Maruyama K., Awazu S., Nishigori H., Iwatsuru M., *Chem. Pharm. Bull.*, **34**, 3394—3402 (1986).
23) Zatón A. M. L., Ferrer J. M., Degordoa J. C. R., Marquínez M. A., *Chem. Biol. Interact.*, **97**, 169—174 (1995).
24) Vorum H., Honoré B., *J. Pharm. Pharmacol.*, **48**, 870—875 (1996).
25) Takamura N., Shinozawa S., Maruyama T., Suenaga A., Otagiri M., *Biol. Pharm. Bull.*, **21**, 174—176 (1998).
26) Chuang V. T. G., Otagiri M., *Pharm. Res.*, **19**, 1458—1464 (2002).
27) Ascenzi P., Bocedi A., Notari S., Fanali G., Fesce R., Fasano M., *Mini Rev. Med. Chem.*, **6**, 483—489 (2006).
28) Fujiwara S., Amisaki T., *Proteins*, **64**, 730—739 (2006).
29) Fujiwara S., Amisaki T., *Biophys. J.*, **94**, 95—103 (2008).
30) Wang J. M., Morin P., Wang W., Kollman P. A., *J. Am. Chem. Soc.*, **123**, 5221—5230 (2001).
31) Berman H. M., Westbrook J., Feng Z., Gilliland G., Bhat T. N., Weissig H., Shindyalov I. N., Bourne P. E., *Nucleic Acids Res.*, **28**, 235—242 (2000).
32) Cornell W. D., Cieplak P., Bayly C. I., Gould I. R., Merz K. M., Ferguson D. M., Spellmeyer D. C., Fox T., Caldwell J. W., Kollman P. A., *J. Am. Chem. Soc.*, **117**, 5179—5197 (1995).
33) Wang J. M., Wolf R. M., Caldwell J. W., Kollman P. A., Case D. A., *J. Comput. Chem.*, **25**, 1157—1174 (2004).
34) Bayly C. I., Cieplak P., Cornell W. D., Kollman P. A., *J. Phys. Chem.*,

97, 10269—10280 (1993).
35) Jorgensen W. L., Chandrasekhar J., Madura J. D., Impey R. W., Klein M. L., *J. Chem. Phys.*, **79**, 926—935 (1983).
36) Darden T., York D., Pedersen L., *J. Chem. Phys.*, **98**, 10089—10092 (1993).
37) Van Gunsteren W. F., Berendsen H. J. C., *Mol. Phys.*, **34**, 1311—1327 (1977).
38) Berendsen H. J. C., Postma J. P. M., Van Gunsteren W. F., DiNola A., Haak J. R., *J. Chem. Phys.*, **81**, 3684—3690 (1984).
39) Humphrey W., Dalke A., Schulten K., *J. Mol. Graphics*, **14**, 33—38 (1996).
40) Honig B., Nicholls A., *Science*, **268**, 1144—1149 (1995).
41) Sitkoff D., Sharp K. A., Honig B., *J. Phys. Chem.*, **98**, 1978—1988 (1994).
42) Kottalam J., Case D. A., *Biopolymers*, **29**, 1409—1421 (1990).
43) Wadelius M., Pirmohamed M., *Pharmacogenomics J.*, **7**, 99—111 (2007).
44) Kragh-Hansen U., *Mol. Pharmacol.*, **34**, 160—171 (1988).
45) Yamasaki K., Maruyama T., Kragh-Hansen U., Otagiri M., *Biochim. Biophys. Acta*, **1295**, 147—157 (1996).
46) Benet L. Z., Hoener B. A., *Clin. Pharmacol. Ther.*, **71**, 115—121 (2002).